Applied Chemical Engineering (2025) Volume 9 Issue 1 ISSN: 2578-2010 (O)
doi: 10.59429/ace.v9i1.5794

ORIGINAL RESEARCH ARTICLE

Formulation and Statistical Optimisation of Liposome-Loaded Glimepiride Using Design-Expert® Software

Wafaa Nahi[1], Sarmad Al-Edresi[2], Rafid Mohammed Ali Hassan wasfi[3]

[1] *Department of Pharmaceutics, Faculty of Pharmacy, University of Al-Qadisiya, Al-Diwaniyah, Iraq.*

[2] *Department of Pharmaceutics and Industrial Pharmacy, Faculty of Pharmacy, University of Kufa, Najaf, Iraq, 52001.*

[3] *Clinical Laboratory Sciences, Faculty of Pharmacy, University of Kufa, Najaf, Iraq.*

***Corresponding author:** Wafaa Nahi;wafaanahi588@gmail.com

ARTICLE INFO

Received: 09 October 2025
Accepted: 04 December 2025
Available online: 04 February 2026

COPYRIGHT

Copyright © 2026 by author(s).
Applied Chemical Engineering is published by Arts and Science Press Pte. Ltd. This work is licensed under the Creative Commons Attribution-NonCommercial 4.0 International License (CC BY 4.0).
https://creativecommons.org/licenses/by/4.0/

ABSTRACT

Background: Glimepiride is a popular third-generation sulfonylurea used to treat type 2 diabetes. Its therapeutic effectiveness is, however, limited by its fluctuating bioavailability and poor water solubility. Liposomal drug delivery techniques offer an attractive means of improving the stability, solubility, and bioavailability of poorly soluble drugs like Glimepiride.

Objective: This study seeks to develop and statistically optimise Glimepiride-loaded liposomes utilising Design-expert® software as part of an extensive pre-formulation analysis.

Method: Liposomes were synthesised utilising the thin-film hydration method, adjusting critical formulation variables like phospholipid content and cholesterol proportion. Utilizing a statistical experimental design methodology, the impact of these factors on key quality measures, including loading capacity (DL%), entrapment efficacy (EE%), zeta potential, particle size, and polydispersity index (PDI), was assessed. The Design-expert ® software facilitated model generation, optimisation, and response surface analysis.

Results: A statistical investigation revealed that the formulation factors had a substantial effect on the liposomes' properties. Zeta potential of -28.85 mV, polydispersity index (PDI) of 0.025, particle size of 71 nm, drug loading (DL%) of 7.53%, and entrapment efficiency (EE%) of 35% were all characteristics of the optimized liposomal formulation. The regression models demonstrated robust predictive capability, and the design space was effectively delineated for subsequent formulation development.

Conclusion: This preformulation study illustrated the successful application of statistical design in optimising Glimepiride-loaded liposomes. These findings establish a foundation for subsequent studies concerning in vitro release and stability testing in the forthcoming phase of formulation development.

Keywords: Liposome; Glimepiride; Preformulation; Design-Expert® software

1. Introduction

Diabetes mellitus (DM), which currently affects 537 million adults, is predicted to increase to 643 million by 2030 and 783 million by 2045, putting hundreds of millions of individuals at serious risk [1]. Type 2 diabetes mellitus (T2DM) is a prevalent global health issue that can lead to kidney failure, heart attacks, strokes, blindness, and lower limb amputations. The disadvantages of conventional drug delivery techniques include suboptimal potency, toxicity, restricted target specificity, and incorrect or insufficient dosages, which might have detrimental side effects on other organs and tissues [2].

In addition to being safe and efficient, management must enhance the patient's quality of life. Although there are a number of novel therapies being investigated, the most urgent need is for drugs that improve insulin sensitivity, stop the growing loss of pancreatic β-cells, and stop or reverse microvascular complications—the main characteristics of type 2 diabetes [3].

Meglitinides, thiazolidinediones, biguanides, sulfonylureas, DPP-4 inhibitors, α-glucosidase inhibitors, and incretin mimetics are among the many kinds of antidiabetic medications that are available. This study focuses on locally accessible Glimepiride (GLM) because of its affordability and capacity to increase the release of insulin from beta cells in the pancreas. It thereby binds to the beta cell's sulfonylurea receptor, triggering a series of processes that culminate in insulin secretion. In contrast to metformin, which predominantly diminishes hepatic glucose synthesis, GLM directly elevates insulin levels. Moreover, it has a comparatively reduced occurrence of gastrointestinal adverse effects about several other antidiabetic medications. GLM is crucial for regulating blood glucose levels by augmenting insulin secretion and mitigating problems related to diabetes[4]. It has limited benefits due to a number of factors, including low bioavailability and poor solubility [5]. Glimepiride is practically insoluble in water and acidic conditions when it comes to solubility, but has high permeability (class II). A controlled drug release method must be developed in order to keep the plasma concentration constant for a long time and prevent hypoglycemia adverse effects, which occur when the medication is released into the bloodstream quickly and subsequently gradually diminished [6].

To address these limitations and sustain a consistent plasma concentration over an extended duration, researchers have explored the application of encapsulated drugs utilizing liposome nanoparticles (NPs) [7]. Liposome nanoparticles exhibit enhanced safety when utilized with physiological substances due to their superior biocompatibility and biodegradability [8].

To improve nanoscale bio-actives, nanoencapsulation techniques and delivery systems can alter the material's surface area, solubility, shape, particle size, size distribution, and sustained release mechanisms, among other chemical and physical properties [9, 10]. The pharmaceutical sector has engineered nanosized medications that exhibit solubility and passive membrane transfer allows for absorption [11, 12].

Pharmaceuticals that are quickly digested and removed from the body after consumption have benefited from this mode of drug administration. Sustained release facilitates the continuous administration of drugs by modulating the rate at which they are introduced into the bloodstream or specific tissues [13]. This delivery system is capable of providing an prolonged therapeutic benefit by gradually releasing the therapeutic material over an extended duration, ranging from days to months, after the administration of a single dose. Their ability to enhance the stability and solubility of pharmaceuticals facilitates more efficient absorption within the body. Furthermore, their diminutive size allows for enhanced penetration of biological barriers, which may result in better treatment outcomes [14].

The administration of sustained release drugs offers numerous advantages compared to conventional dosage forms, such as an increased safety margin for potent medications, reduced volatility, and improved patient adherence [15]. Often, polymers, coatings, or matrix systems that control the drug's rate of absorption

and dissolution within the body are used to do this [16]. Sustained release formulations maintain a steady level of drug in the circulation, minimizing fluctuations in drug levels, thereby lowering the possibility of adverse effects and improving treatment results [17]. A sustained-release dose form of the GLM drug (coated medicine in capsules) has recently been developed to allow for less frequent administration [18].

Liposomes serve as effective models for biological membranes [19] and effective vehicles for drug delivery. One or more phospholipid bilayers encircle the aqueous core of microscopic spherical vesicles. The formation of these structures occurs when lipids are dispersed in an aqueous medium, leading to the creation of vesicles that vary in size from 30 nm to several micrometers [20, 21]. By enabling focused medication administration and controlled release, liposomes improve therapeutic effectiveness and lower the frequency of doses. Numerous substances, including drugs, bacteria, viruses, antigens, peptides, antibiotics, vaccines, DNA, and diagnostic agents, have been transported via them [22]. Drug loading occurs either actively after liposome production or passively during liposome development, and the preparation techniques include sonication, solvent dispersion, thin-film hydration, and detergent removal [23].

They fall into one of two categories: multilamellar vesicles (MLV) or unilamellar vesicles (ULV), which are further divided into large unilamellar vesicles (LUV) and small unilamellar vesicles (SUV) [24, 25]. The size and number of bilayers affect encapsulation efficiency and circulation half-life.

Liposomal formulations typically exhibit decreased systemic toxicity while preserving or enhancing therapeutic efficacy, underscoring their significance in contemporary delivery systems [26].

This research focused on formulating Glimepiride by encapsulating it in liposomes created from a lipid mixture, utilizing Design-Expert® software for optimization.

2. Materials and methods

2.1. Materials

DSPC, DPPC, cholesterol, and glimepiride powder were purchased from Hyperchem in China. In Germany, BASF sold Soluplus® to the company. The sodium hydrogen phosphate (Na2HPO4) and potassium dihydrogen phosphate (KH2PO4) were supplied by Thomas Baker in India. The supplier of sodium chloride (NaCl) was LAD in India. We acquired organic solvents from Chemlab in Belgium..

3. Methods

3.1. Melting point determination

Glimepiride powder's melting point was ascertained by adding a tiny amount of the powdered medication to a capillary glass tube that was open at one end and sealed at the other. After that, the tube was placed inside a digital melting point device, and the temperature at which the medication powder completely melted was noted [27].

3.2. Saturated solubility of Glimepiride

The shaking flask method was used to evaluate Glimepiride's saturation solubility in various solutions (Albo Hamrah et al. 2020). In a test tube, 10 mL of different solvents were mixed with an excess of glimepiride powder separately. The sealed tubes underwent shaking for a duration of 48 hours at a temperature of 25 ± 0.5°C. To evaluate the drug particles' precipitation in the sample, a visual examination was performed. A 0.45µm filter paper was used to filter a part of the solution, and the HPLC method was used to evaluate the filtrate. Glimepiride's solubility in organic solvents such as ethanol, methanol, and acetonitrile, as well as in water and phosphate buffers at pH 7.4 and 6.8, was evaluated in three different ways.

3.3. HPLC operating parameters for glimepiride assay

High-pressure liquid chromatography (HPLC) with a Shimadzu UFLC Prestige HPLC system (Koya, Japan) was used to examine glimepiride. At a wavelength of 228 nm, a PDA detector (SPD20A) was used, and a manual injector was adjusted for an injection volume of 10 µl. The mobile phase, which included acetonitrile and water in a 70:30 v/v ratio, was delivered at a flow rate of one milliliter per minute. At room temperature, a Gemini C18 column with dimensions of 100 × 4.6 mm (ID) and 5 µm was used to separate the medication. Prior to application, the mobile phase was degassed and passed through a 0.45-µm membrane filter.

3.4. Construction calibration curves of Glimepiride

A stock solution with a concentration of 100 µg/ml has to be prepared for this procedure. After transferring 10 mg of GLM into a 100 ml volumetric flask, the mobile phase was added, and the mixture was sonicated to achieve this. Aluminum foil was used to protect the stock solution from light. Standard stock solution aliquots of GLM were put into 10-mL volumetric flasks using A-grade bulb pipettes. The final concentrations of 10, 20, 30, 40, 50, and 60 µg/ml were attained by adjusting the solutions to volume using the mobile phase. HPLC was utilized to analyze the solutions using the recommended method, and the calibration curve was produced by charting the outcomes against concentrations. The calibration curve was constructed in order to calculate the calibration curve equation and the regression coefficient (R^2) value.

3.5. Validation of the method

The optimized chromatographic method was fully validated by the procedures outlined in ICH guidelines Q2 (R1) for the validation of analytical methods.

Table 1. Chromatographic settings that are optimized.

Phase of stationery (column)	**Phenomenex Luna C1 (250 x 4.5 mm) with particles of size 5 µm**
Mobile phase	Acetonitrile, water 70:30 (v/v)
Detection wavelength (nm)	228
Glimepiride R_t (min)	6
Flow rate (ml/min)	1
Column temperature	Ambient
Volume of injection (µL)	10
Run time (min)	15

3.6. Range and linearity

A range of concentrations, from 10 to 60 µg/ml of GLM, were obtained by diluting the standard stock solution. The solutions were injected into the HPLC column three times with a fixed injection volume of 10 µl.

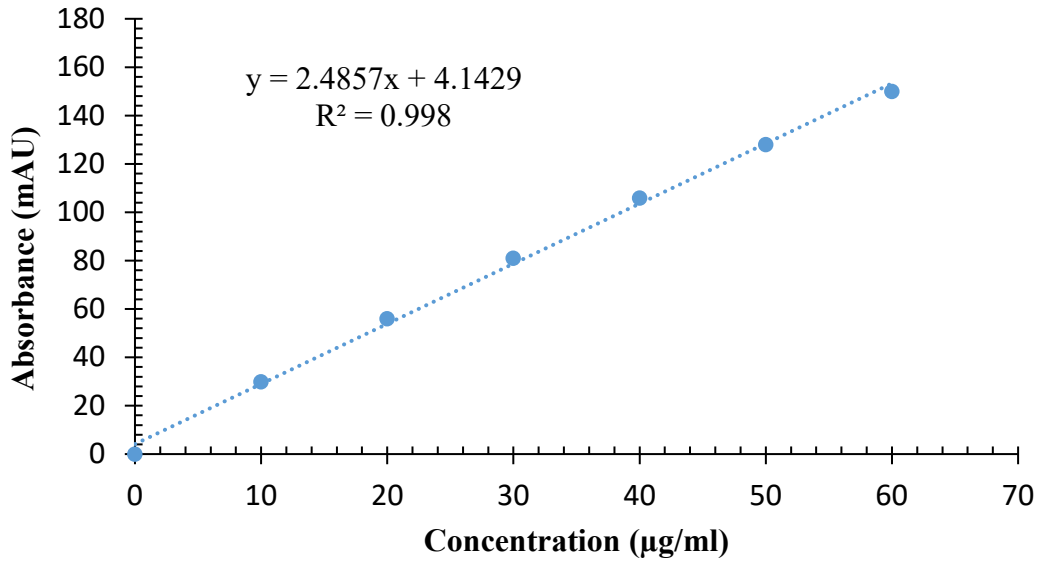

Figure 1. Calibration curve of Glimepiride in acetonitrile: water (70:30 v/v) as mobile phase. Glimepiride was dissolved in the mobile phase at concentrations of 10, 20, 30, 40, 50, and 60 µg/ml. Data are expressed as mean ± standard deviation from six independent experiments.

3.7. Precision

Three injections at different doses (10–60 µg/ml) were administered on the same day in order to assess intra-day accuracy, and the percentage relative standard deviation (%RSD) values were calculated. The investigations were conducted across a number of days in order to evaluate inter-day accuracy.

3.8. Accuracy

To conduct a preliminary accuracy assessment, a standard solution of Glimepiride was made at a concentration of 20 µg/ml. Triplicate administration of the solution was carried out under the specified chromatographic conditions.

Table 2. The Glimepiride linearity parameter in acetonitrile: water (70:30 v/v) as the mobile phase.

Concentration of Glimepiride (µg/ml)	Absorbance of Glimepiride (mAU)
10	30
20	56
30	81
40	106
50	128
60	150

3.9. Limit of quantification and limit of detection

The limit of quantification (LOQ) was determined to be the lowest plasma concentration on the standard curve that could be measured with a respectable degree of accuracy and precision. The smallest amount of analyte that can be detected in a sample under the given experimental circumstances, even if it might not be measurable, is known as the limit of detection (LOD). The determination is based on statistical methods utilizing the standard deviation of the residuals, as outlined in eqs. 1 and 2 and table 3:

$$LOD=3.3\times(SD/Slope) \quad (1)$$

$$LOQ=10\times(SD/Slope) \quad (2)$$

Table 3. Precision information assessed by intra- and inter-day research.

Concentration (µg/ml)	Intra-day (n = 3)		Inter-day (n = 3)	
	average peak area (n = 3) ± SD	%RSD	average peak area (n = 3) ± SD	%RSD
20	56.5±0.8	1.4	56±1	1.7
30	81.7±1.4	1.8	81.6±1.5	1.8
40	106±1.5	1.4	105±1.1	1
50	131±2.6	2	125.5±1.5	1.1
60	151.5±2.29	1.5	148±2.6	1.7

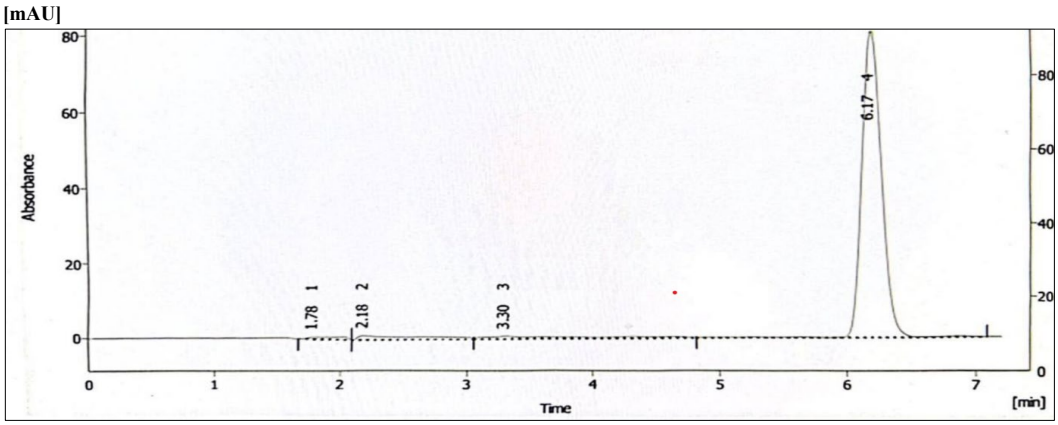

Figure 2. Glimepiride's HPLC chromatogram with acetonitrile: water (70:30 v/v) as the mobile phase, a detection wavelength of 228 nm, a retention period of around 6 minutes, and a flow rate of 1 ml/min.

3.10. Preparation of liposome-loaded Glimepiride

Glimepiride-loaded liposomes were synthesized utilizing the thin film rehydration method. A chloroform: methanol combination (2:1) was used to dissolve glimepiride, DSPC, DPPC, and cholesterol in a round-bottom flask. At 50 mm Hg and 60 °C, the organic solvents were evaporated for at least 30 minutes using a rotary evaporator. A homogenizer was then used to resuspend the leftover film in 10 milliliters of phosphate buffer at pH 7.4. Consequently, liposomes began to form concurrently.

3.11. Optimizing the formulation with a factorial design

Particle size, PDI, zeta potential, EE%, and DL% were the response variables that were optimized using a complete factorial design that included three components (DSPC, DPPC, and cholesterol). The optimal concentrations of DSPC, DPPC, and cholesterol required for liposome formation were identified based on the most favorable responses. The concentrations of A (DPPC), B (DSPC), and C (cholesterol) were among the independent variables. The dependent variables contained the following: The variables for the responses were R1 (particle size), R2 (PDI), R3 (zeta potential), R4 (EE%), and R5 (DL%). Three variables at three different concentration levels were assessed in this design: low (8 mg), medium (20 mg), and high (40 mg). This design made use of the factors, which are represented by the codes -1, 0, and +1. Experiments were carried out for every conceivable combination. Consequently, to encompass the whole range of experiments included in Table 4, seventeen suggested runs were produced. To assess the lack of fit and identify potential human errors, specific experiments at identical doses were replicated with Design-Expert® software. Throughout the trial, other characteristics related to formulation processing stayed unchanged.

Table 4. The 2^3factorial design of glimepiride-loaded liposomes.

Run	DPPC (A)	DSPC (B)	Cholesterol (C)
1	-1	-1	1
2	-1	1	1
3	1	-1	-1
4	1	1	1
5	-1	-1	-1
6	1	1	-1
7	1	-1	1
8	1	1	-1
9	-1	-1	-1
10	-1	1	1
11	1	-1	-1
12	1	-1	1
13	-1	1	-1
14	-1	1	-1
15	-1	-1	1
16	1	1	1
17	0	0	0

A detailed analysis of the independent factors' effects on the response was conducted. Eq. 3 was used to build the response regression equation.

$$Y = b_0 + b_1A + b_2B + b_3C + b_4AB + b_5AC + b_6BC \quad (3)$$

The quantitative impact of the independent variables is represented by Y, whereas the regression coefficient for the independent variables A, B, and C is shown by b. Altering a single variable sequentially (average outcomes) illustrates the primary impact of (A, B, and C) from its lowest to its highest value.

3.12. Data analysis and the desirable function

Using Design-Expert® software (Version 13, Stat-Ease Inc., Minneapolis, MN), several response surface methodology (RSM) analyses were employed in this optimization study. Three factorial designs were created for each response using the factorial models. The Design-Expert® program was used to create three-dimensional charts. The chosen factors' significance on the variables was assessed using a two-way analysis of variance (ANOVA). After the mathematical optimization model was fitted, the desirability function was applied. Combining replies was part of the optimization process to find a highly desirable product. The desirability function aggregated all of the responses into a single variable in order to forecast the optimal levels of the independent variables. The desirability rating ranged from 0 to 1. For this reason, zero is an unsatisfactory answer, whereas one is the best possible result. After preparing the optimum formulation chosen by the design, a comparison between the design's anticipated and observed values was made.

3.13. Analysis of particle size and polydispersity index

Angstrom Advance Inc.'s ABT-9000 nano laser particle size analyzer, which is a dynamic light scattering instrument, was used to measure the particle size. Without diluting the samples, it uses a scattering angle of 90° and a constant temperature of 25°C to quantify the intensity of light scattered by the sample molecules over time. Analyzing samples of formulae in the analyzer allows one to identify the particle size. For every formulation, measurements were made of the samples' average diameters and polydispersity indices.

Monodispersity is indicated by a low polydispersity index, whereas a broad particle size distribution is indicated by a high index. The following categories apply to the values of the Polydispersity Index (PDI): A PDI between 0 and 0.05 denotes monodispersity, 0.05 and 0.7 is thought to be ideal for homogeneity and uniform particle distribution, while a PDI over 0.7 but below one denotes a wide particle size distribution [28].

3.14. Determination of entrapment efficiency (EE%) of Glimepiride

High-Performance Liquid Chromatography (HPLC) techniques are employed for the quantification of pharmaceutical compounds. Drug molecules and other fluorescent probes used to measure the effectiveness of liposome penetration may be resolved and detected with greater precision and accuracy using the HPLC approach. The unentrapped and entrapped drugs are separated for examination using the drug encapsulated centrifugation process. Freshly prepared liposomes with varying drug-to-lipid ratios were subjected to centrifugation using a cooled ultracentrifuge at around 20,000 rpm for 20 minutes at 4°C. Subsequently, the liposome vesicles are disrupted using methanol. Using the HPLC method and the following formula, the solution's percentage entrapment efficiency (%EE) is determined [29].

$$\% \text{ EE} = \frac{concentration\ of\ drug\ entraped}{concentration\ of\ theoretical\ drug} \text{ x } 100 \quad (4)$$

3.15. Formulation and assessment of the optimized recipe

After nine trials, the Design-Expert® program produced an ideal formula with an emphasis on boosting EE% while lowering particle size and polydispersity index. After comparing the created index with the resultant suggestions, a number ranging from 0 to 1 was obtained. Upon setting the criteria, the optimal formula was selected [30].

3.16. FTIR-based drug-excipient compatibility studies

The qualitative estimate and identification of the compound's functional groups were made easier by the FTIR analysis. GMP was integrated with the components in an appropriate ratio, in alignment with that utilized in the formulation process. The FTIR analysis was conducted to obtain spectra of pure Glimepiride and the physical mixture. The spectra acquired spanned from 4000 to 400 cm−1, with a resolution of 2 cm^{-1}, employing a Nicolet Avatar 370 instrument (Thermo Nicolet Corporation, USA) [31, 32].

3.17. Statistical analysis

Statistical analyses were performed utilizing Design-Expert® software version 13. A p-value of less than or equal to 0.05 was noted. Microsoft Excel 2020 was used to calculate means and standard deviations, and the results were displayed as mean ± standard deviation. Data were normalized to percentages as required, and evaluations were conducted regarding the regulatory condition.

4. Results and discussion

4.1. Glimepiride melting point

The melting point of Glimepiride is recorded as ranging from 205 °C to 209 °C. The experiment's results aligned with those reported by Lakumalla et al. (2024), which indicated that pure glimepiride powder melts at 205–209 °C [33].

4.2. Saturated solubility of Glimepiride

Table 5 presents the results of the saturated solubility of Glimepiride. According to the study, Glimepiride becomes more soluble when pH levels rise. Gandhi et al. (2023) and Paul, Roy et al. (2020) have reported comparable results [34-36].

Table 5. Glimepiride's solubility in various solvents.

Solvent	Solubility (mg/ml)
Water	0.0038
Acetonitrile	0.46
Methanol	0.58
6.8PH buffer	0.0037
7.4 PH buffer	0.00863

4.3. Method development

The development of new HPLC methods is beneficial for routine quality control assessments of pharmaceuticals, providing essential information for optimizing experimental conditions to enhance drug utilization. This study offers a developed and validated RP-HPLC technique that complies with ICH requirements for accuracy, specificity, and selectivity in measuring and assessing the drug release profile of GLM. Various proportions of acetonitrile and water were tested, ultimately leading to the selection of a 70:30 v/v ratio of acetonitrile to water, this supplied appropriate system suitability characteristics and a satisfactory resolution. The chromatogram of the GLM solution's working standard is shown in figure 2. Table 1 presents the optimized chromatographic conditions. Prior to application, a 0.45-µm membrane filter was used to filter the mobile phase. Following the transfer of the contents to the solvent reservoir of the LC20AD pump, the solvent line was purged using 30 milliliters of fresh mobile phase.

4.4. Linearity

The stock solution was used to create new test samples with concentrations ranging from 10 to 60 µg/ml of (GLM). Three injections of each concentration were made, and the outcomes were analyzed in optimal chromatographic circumstances. Plotting the drug concentration against the response (peak height) produced a calibration curve, as shown in Figure 1. Table 2 presents the linearity parameter for the Generalized Linear Model (GLM).

4.5. Precision

Experiments on intra- and inter-day variance validated the accuracy of the approach. The standard and sample solutions were analyzed three times in a single day for the intra-day analyses, and the response factor's percentage RSD was calculated; the findings are displayed in Table 3. The %RSD values in both cases were ≤ 2%, demonstrating adequate precision of the approach, in accordance with the results of Mohd, Sanka et al. (2014) [37].

4.6. Accuracy

The mean assessed concentration of the 20 µg/ml standard solution approximated the nominal value, with a recovery percentage residing within the permissible range (often 98-102%). This validates the method's capacity to yield precise results at this concentration level.

4.7. Limit of quantification and limit of detection

A concentration of 100 µg/ml was used to create standard stock solutions of GLM. Standard stock solutions were diluted with the mobile phase to create standard solutions of GLM at concentrations of 10, 20, 30, 40, 50, and 60 µg/ml. Statistical techniques using the standard deviation of the residuals were used to determine the detection limits (LOD) and quantification limits (LOQ) for the generalized linear model (GLM) under the current chromatographic circumstances. For GLM, the quantification (LOQ) and detection (LOD) limits were set at 3.58 µg/ml and 1.18 µg/ml, respectively.

4.8. FTIR drug-excipient compatibility studies

Pure Glimepiride displayed peaks at 3368.77 cm^{-1} and 3288 cm^{-1}, which are associated with N-H stretching of the secondary amine, and at 2931.94 cm^{-1}, relating to aromatic C-H stretching, as illustrated in Fig. 3a. Peaks at 1704.93 cm^{-1}, ascribed to ester C=O stretching, and at 1345.42 cm−1, relating to O=S=O stretching. Table 5 outlines the functional groups that account for the unique peaks of GMP. The experimental results corresponded with the observations of Kishore and his associates (2013), who identified analogous FTIR peaks [38].

The FTIR spectra of the physical mixture exhibited peaks at 3371.57 cm^{-1}, 3290.56 cm^{-1}, 2920.23 cm^{-1}, 1735.93 cm^{-1}, and 1672.28 cm-1, corresponding to N-H stretching (secondary amine), aromatic C-H stretching, C=O stretching, N-C=O stretching, and O=S=O stretching of Glimepiride, respectively (Fig. 3b; Table 6).

The FTIR spectra of the drug in conjunction with other lipids exhibited characteristic peaks within the specified range. FTIR spectral analysis indicated that there were no changes in the distinctive peaks of pure Glimepiride in the physical mixture, as shown in Fig. 3b.

The findings demonstrate that there is no chemical interaction between the drug and lipids, suggesting that Glimepiride is compatible with the formulation's excipients.

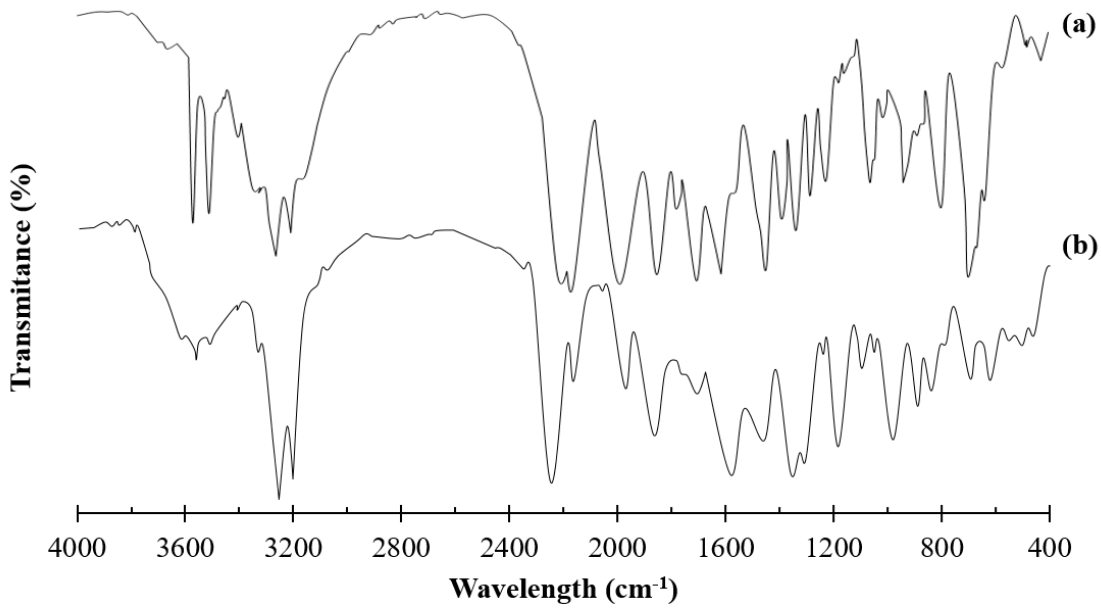

Figure 3. The infrared Fourier transform spectra of (a) glimepiride and (b) glimepiride-lipid compound.

Table 6. Glimepiride bending and stretching.

Wave number peak (cm^{-1})	Interpretation	Frequency
3368.77, 3288	N-H stretch (Secondary amine)	3700-3000
2931.94	C-H stretch (aliphatic)	1500-1300
1704.93	C=O stretch	1900-1590
1345.42	O=S=O	1140-1350

Table 7. FTIR drug-excipient compatibility studies.

Glimepiride X(cm^{-1})	Glimepiride+ lipid mixture X(cm^{-1})	Interpretation
3369.64	3371.57	N-H stretch (Secondary amine)
3288	3290.56	N-H stretch (Secondary amine)
2931.94	2920.23	C-H stretch (aliphatic)

Glimepiride X(cm^{-1})	Glimepiride+ lipid mixture X(cm^{-1})	Interpretation
1704.93	1735.93	C=O stretch
1670.95	1672.28	N-C=O stretch
1345.42	1346.31	O=S=O

Table 7. (*Continued*)

4.9. Analysis of particle size, PDI, DL% and EE%,

The results showed that the produced liposomes' particle sizes ranged from 45 nm to 100 nm. The variations in particle sizes are associated with lipid concentrations, particularly the type and concentration of phospholipids and cholesterol utilized [39]. According to Table 7, the lowest particle size measured in Run 2 was 45 nm, while the largest was 100 nm in Run 1. The smaller particle size observed in DSPC-based liposomes can be explained by the increased membrane rigidity and denser molecular packing due to the longer acyl chains of DSPC, promoting more compact vesicle formation [40].

The polydispersity index (PDI) values varied between 0.01 and 0.07, suggesting particle populations that are uniform to moderately dispersed. Run 16 demonstrated a monodisperse polydispersity index (PDI) of 0.019, in contrast to run 3, which exhibited a broader distribution with a PDI of 0.07. Run 17 exhibited a moderate PDI [41, 42].

Entrapment efficiency (EE%) exhibited variability across formulations, with values ranging from 35% to 55%. Run 9 recorded the highest EE% at 55%. In contrast, lower EE% values were observed, such as 35% in run 16. The observed variations in EE% can be ascribed to the differing lipid compositions utilized in the formulation. Specifically, DPPC and cholesterol exhibited a comparable diminishing effect on EE%, whereas DSPC demonstrated a slight adverse effect. These reductions due to EE% may be related to increased bilayer rigidity or reduced space for drug encapsulation due to tighter membrane packing [43].

Table 8. Responses parameters obtained from the 2^3factorial design of Glimepiride-loaded liposomes' formulations.

Run	particle size(nm) (R1)	PDI (R2)	zeta potential (R3)	DL% (R4)	EE% (R5)
1	100	0.029	-55	9.37	45
2	45	0.024	-35.3	9.13	53
3	76	0.07	-3.9	8.7	54
4	76.7	0.022	-24	6.9	54
5	58	0.03	0.5	11.9	50
6	70.9	0.031	-90	6.1	44
7	85.8	0.023	106.8	7.35	50
8	77	0.03	41.5	6.25	45
9	66	0.03	-6.3	13.9	55
10	46.9	0.023	-69	8.62	50
11	78.5	0.02	0.1	8.22	51
12	86	0.02	0.3	5.58	38
13	87.6	0.02	-4.8	9.61	50
14	87.8	0.03	-55.5	9.23	48
15	99	0.03	45.5	8.75	42
16	77	0.019	0.2	4.48	35
17	69	0.02	98.5	7.3	44

The DL% results varied from 4.48% in Run 16 to 13.9% in Run 9, as presented in Table 7. The DL% increased with a decrease in lipid concentration.

4.10. Experimental design and analysis

The analysis of the data presented in Table 8 was conducted using the Design-Expert® software and fit statistics. Parameters were obtained, encompassing the p-value, adjusted determination coefficient (adj. R2), projected determination coefficient (pred. R2), and ANOVA for all responses. The p-values obtained were 0.0733 for R1, 0.5073 for R2, 0.6807 for R3 (i.e., ≤ 0.05), 0.0002 for R4, and 0.3518 for R5. This suggests that only the R4 model demonstrated significance. This response is strongly influenced by the three lipids.

Table 9. Evaluation of the fit statistics for the outputs generated by Design-Expert® software.

Parameters	Particle size	PDI	Zeta potential	DL%	EE%
Standard deviation	12.06	0.0119	57.11	0.9440	5.45
Mean	75.72	0.0277	-2.96	8.32	47.53
C.V.%	15.93	43.10	1926.30	11.35	11.46
R^2	0.6260	0.3609	0.2851	0.8940	0.4323
Adj. R^2	0.4015	-0.0225	-0.1439	0.8305	0.0916
Pred. R^2	-0.1437	-0.9407	-0.7811	0.6939	-0.7236
Adeq. precision	5.1620	3.1971	2.8843	11.1660	2.6474
P-value	0.0733	0.5073	0.6807	0.0002	0.3518

The experimental setup was a 17-run factorial design with three factors at three levels, represented by the symbols -1, 0, and +1. This indicates an efficient first-order design requiring a limited number of experiments. The impact of individual variables was recognized as the primary effect. Additionally, The response surface was established, providing further benefits to this design. A full factorial design was utilized to investigate the factors systematically.

The impact on particle size (R1) was determined to be non-significant according to ANOVA, as indicated in Eq. 5.

$$R_1=75.7176+2.35A-5.025B+0.9125C+1.9375AB+1.975AC-10.625BC \quad (5)$$

The negative coefficient of factor B (DSPC) in Eq. 5 indicates that an increase in the concentration of B results in a reduction in particle size. The results of this study correspond with those reported by Mandlik and Ranpise (2017), who demonstrated that chitosan concentration exerted a more significant influence on nanoparticle size than STPP [44].

The 3D response surface plots demonstrated a rise in particle size at diminished concentrations, as depicted in Figure 4a. The reduction in particle size was ascribed to increased concentrations of DSPC, which is characterized by its ability to form more rigid and highly ordered lipid bilayers, a consequence of its long saturated acyl chains and elevated transition temperature. A more compact bilayer structure diminishes the propensity for vesicle aggregation and expansion, resulting in smaller and more uniform nanoparticles [45-47].

The ANOVA analysis indicated that the effect on PDI (R^2) was non-significant, as indicated in Eq. 6.

$$R_2=0.0277059+0.0011875A-0.0033125B-0.0044375C-0.0005625AB-0.0039375AC+0.0015625BC \quad (6)$$

The PDI, indicative of size uniformity, exhibited a greater dependence on lipid concentration, particularly on DSPC and cholesterol. The results demonstrate a decrease in PDI with increasing concentrations of DSPC and cholesterol, as confirmed by the negative charge described in Eq.5. Improved homogeneity was the outcome of decreasing PDI; however, fewer homogenous particles were seen at higher DSPC and cholesterol concentrations. The 3D response surface plots show that the PDI reaches its higher value at low concentrations,

as depicted in Fig. 4b. The findings align with Martins et al. (2011), indicating that higher concentrations of lipids or stabilizers enhance particle uniformity and reduce PDI values [48].

The ANOVA analysis indicated that the effect on zeta potential (R3) was found to be non-significant, as indicated in Eq.7.

$$R3=-2.96471+13.1812A-20.3062B+5.49375C-1.64375AB+11.4563AC-7.90625BC \quad (7)$$

Lipid A exhibited a positive correlation with the coefficient, while lipid B showed a negative correlation. This suggests that the zeta potential increases with higher concentrations of lipid A and decreases with higher concentrations of lipid B. The 3D response surface plots (Figure 4c) demonstrated a linear increase in zeta potential corresponding to higher concentrations of lipid (A).

The ANOVA study revealed a significant effect on DL% (R4), as demonstrated in the eq. 8.

$$R4=8.31706-1.68313A- 0.840625B-0.858125C+0.075625AB+0.238125AC+ 0.600625BC \quad (8)$$

The analysis of DL% (R4) indicated that the coefficient for lipids A, B, and C is negative. This suggests that a drop in DL% would result from an increase in lipid concentration. As shown in Figure 4d, the 3D response surface plots showed that at low lipid concentration, the DL% approaches the upper limit.

The ANOVA analysis revealed a significant effect on EE% (R5), as demonstrated in Eq. 9.

$$R5=47.5294 - 1.375A - 0.375B - 1.875C - 1.5AB - 0.25AC + 2.5BC \quad (9)$$

The negative coefficient for phospholipid A indicates a decrease in EE% with increasing DPPC concentration. This can be attributed to the rigid, saturated phospholipid structure of DPPC (T_m~41 °C), which, when present in excess, reduces bilayer flexibility and internal aqueous volume, thereby limiting drug encapsulation.

The coefficient for DSPC (B) was numerically smaller (–0.3750), indicating a weaker direct effect. The 3D response plot indicated a significant decrease in EE% as DPPC concentration increased, especially at elevated levels. Cholesterol (C) exhibited the most significant individual negative impact, aligning with its established function in diminishing membrane permeability and compressing bilayer structures. Excess cholesterol can restrict internal volume and reduce the fluidity required for efficient drug entrapment.

The interaction term BC (DSPC × Cholesterol) demonstrated a significant positive effect (+2.50), indicating a compensatory or synergistic relationship. The use of DSPC or cholesterol individually decreases EE%, whereas their combination may enhance bilayer stability and optimize structural integrity, leading to improved entrapment. This nonlinear behavior underscores the significance of a balanced formulation design over the individual contributions of each lipid.

The findings corroborate previous studies highlighting the significance of lipid ratios in attaining optimal entrapment efficiency in liposomes [49]. According to the 3D response surface plots, EE% attains its maximum value at lower concentrations, as depicted in Figure 4e.

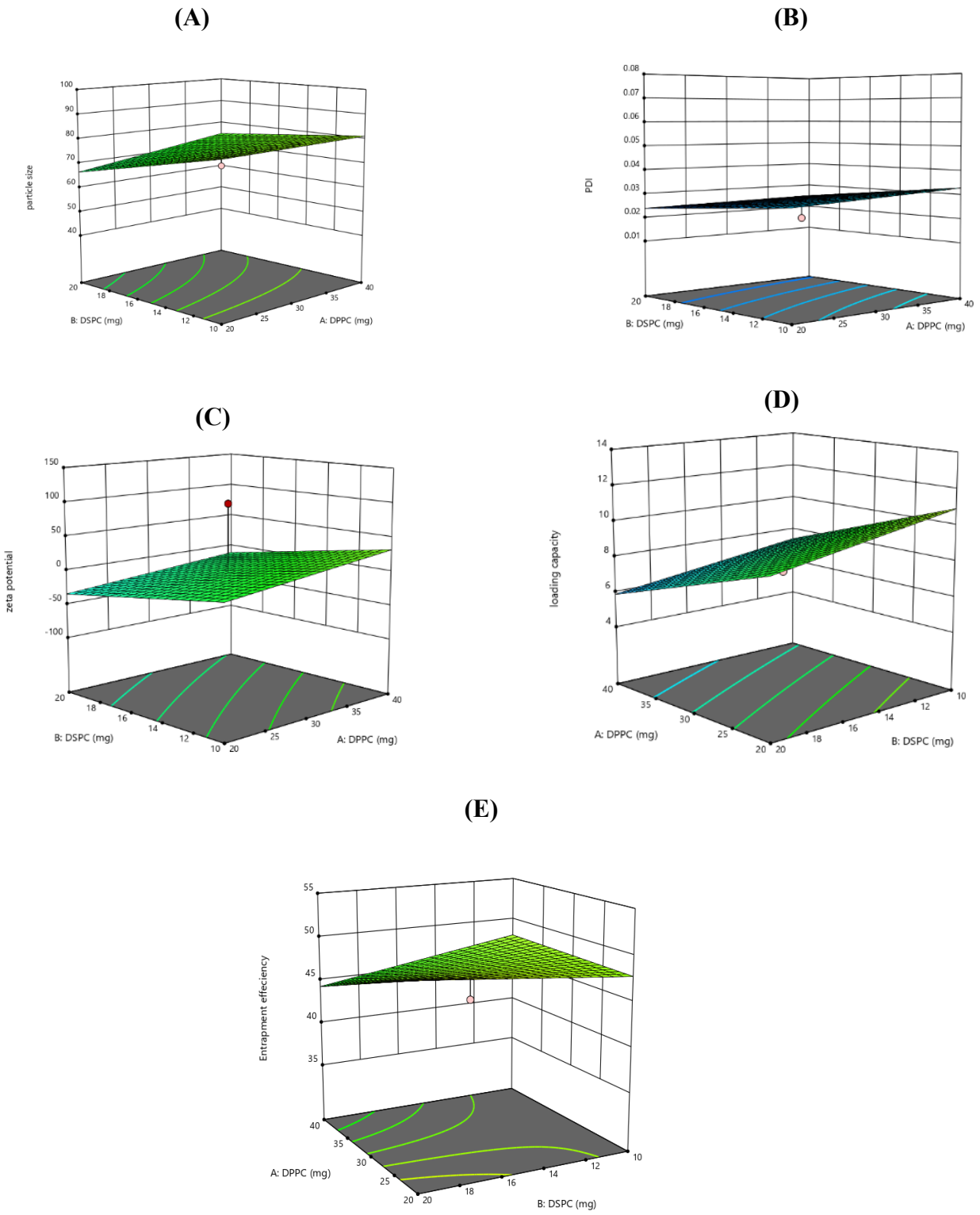

Figure 4. Three-dimensional response surface graphs illustrating the influence of independent variables on dependent variables through (A) particle size, (B) polydispersity index (PDI), (C) zeta potential, (D) drug loading percentage (DL%), and (E) encapsulation efficiency percentage (EE%) generated using Design-Expert® software.

4.11. Optimization and evaluation of the formulated products

Optimization seeks to identify the critical variables that substantially influence the chosen responses and to ascertain the optimal levels of these variables to yield a high-quality and consistent outcome [50]. Responses that affect the quality of the product must be taken into account during the optimization process. The reaction

criteria included a particle size range of 70-100 nm, a PDI greater than 0.1, a zeta potential of less than -30 mV, maximized EE%, and a DL of less than a specified value. Responses from the factorial formulation indicated the use of 20 mg, 15 mg, and 8 mg of DPPC, DSPC, and cholesterol, respectively. The predicted particle size was 70.39 nm, with a PDI of 0.026, a zeta potential of -25, a DL% of 8.87%, and an EE% of 47.67. The prepared optimized formulation yielded observed values that closely aligned with the anticipated values. The measured particle size was found to be 71 nm, with a PDI of 0.025, a zeta potential of -28.85, an EE% of 35, and a DL% of 7.53. The relative errors of experimental and expected values are determined using Eq. 10.

$$\text{Relative error} = \frac{(\text{expected} - \text{experimental})}{\text{expected}} \quad (10)$$

The calculated particle size relative error amounted 0.007, the polydispersity index (PDI) was 0.03, the zeta potential was 0.15, the percentage of drug loading (DL%) was 0.1, and the encapsulation efficiency (EE%) was 0.2, indicating a concordance between expected and experimental values. The results of this investigation validate the confirmed feasibility of the model [51].

5. Conclusion

This formulation study effectively demonstrated the development and statistical optimization of Glimepiride-loaded liposomes utilizing Design-Expert® software. The loading capacity model showed the most favorable statistical fit among the evaluated responses, underscoring the impact of formulation variables on entrapment behavior. The models for particle size and other responses exhibited moderate to weak fitting; however, the defined design space provides a robust foundation for further refinement. These findings establish a basis for future work focused on *in vitro* release, stability assessments, and eventual *in vivo* evaluations.

Conflict of interest

The authors declare no conflict of interest

References

1. Soomro, M.H. and A. Jabbar, *Chapter 2 - Diabetes etiopathology, classification, diagnosis, and epidemiology*, in *BIDE' s Diabetes Desk Book*, A. Basit and M.Y. Ahmedani, Editors. 2024, Elsevier. p. 19-42.
2. Mohan, L., C. Anandan, and N. Rajendran, *Drug release characteristics of quercetin-loaded TiO2 nanotubes coated with chitosan.* International Journal of Biological Macromolecules, 2016. **93**: p. 1633-1638.
3. Donath, M.Y., C.A. Dinarello, and T. Mandrup-Poulsen, *Targeting innate immune mediators in type 1 and type 2 diabetes.* Nature Reviews Immunology, 2019. **19**(12): p. 734-746.
4. Lorenzati, B., et al., *Oral Hypoglycemic Drugs: Pathophysiological Basis of Their Mechanism of ActionOral Hypoglycemic Drugs: Pathophysiological Basis of Their Mechanism of Action.* Pharmaceuticals, 2010. **3**(9): p. 3005-3020.
5. He, W., et al., *Glimepiride use is associated with reduced cardiovascular mortality in patients with type 2 diabetes and chronic heart failure: a prospective cohort study.* European Journal of Preventive Cardiology, 2022. **30**(6): p. 474-487.
6. Chandran, M.P. and V.P. Pandey, *Formulation and evaluation of glimepiride-loaded liposomes by ethanol-injection method.* 2016. **9**: p. 192-195.
7. Al-Janabi ma and Al-Edresi ss, *Preparation and validation of nanofibers loaded with silver sulfadiazine from zein/poly (Ɛ -caprolactone)/poly (ethylene oxide) for topical dosage forms to improve release behaviour.* J.Res.Pharm., 2024. **28**(6): p. 2114-2125.
8. Mohammadpour, F., et al., *Preparation, in vitro and in vivo evaluation of PLGA/Chitosan based nano-complex as a novel insulin delivery formulation.* International Journal of Pharmaceutics, 2019. **572**: p. 118710.
9. Ubeyitogullari, A., et al., *Polysaccharide-based porous biopolymers for enhanced bioaccessibility and bioavailability of bioactive food compounds: Challenges, advances, and opportunities.* Comprehensive Reviews in Food Science and Food Safety, 2022. **21**(6): p. 4610-4639.
10. Al-Edresi, S., K. Albo Hamrah, and A. Al-Shaibani, *Formulation and validation of Candesartan cilexetil-loaded nanosuspension to enhance solubility.* Pharmacia, 2024. **71**: p. 1-13.
11. Karthick, V., et al., *Optimization and characterization of eco-friendly formulated ZnO NPs in various parameters: assessment of its antidiabetic, antioxidant and antibacterial properties.* Biomass Conversion and Biorefinery, 2023. **14**: p. 24567-24581.

12. Abd El-Hameed, A.M., et al., *Novel di-aryl chalcone derived pyrazole linked to methane sulfonyl pharmacophore as potent selective COX-2 inhibitors; design, synthesis, molecular modeling, in vitro and in vivo anti-inflammatory activities.* Future Med Chem, 2025. **17**(15): p. 1849-1865.
13. Cong, Y.-Y., et al., *Implantable sustained-release drug delivery systems: a revolution for ocular therapeutics.* International Ophthalmology, 2023. **43**(7): p. 2575-2588.
14. Rajput, A., et al., *A current era in pulsatile drug delivery system: Drug journey based on chronobiology.* Heliyon, 2024.
15. Atiyah, S.R. and S. Al-Edresi, *Preparation And Characterization of Polyvinyl Alcohol Nanofiber Loaded With Mafenide For Sustain Release.* Journal Port Science Research, 2024. **7**(1): p. 43 -50.
16. R. Atiyah, S. and S. Al-Edresi, *PREPARATION AND JUSTIFICATION OF NANOFIBRES-LOADED MAFENIDE USING ELECTROSPINNING TECHNIQUE TO CONTROL RELEASE.* International Journal of Applied Pharmaceutics, 2024. **16**(2): p. 224-230.
17. Al-Edresi, S., M.T. Abdul-Hasan, and Y.A. Hadi Salal, *Formulation, analysis and validation of nanosuspensions-loaded voriconazole to enhance solubility.* International Journal of Applied Pharmaceutics, 2024. **16**(2): p. 209-214.
18. Janczura, M., S. Sip, and J. Cielecka-Piontek, *The Development of Innovative Dosage Forms of the Fixed-Dose Combination of Active Pharmaceutical Ingredients.* Pharmaceutics, 2022. **14**(4): p. 834.
19. AlEdresi, S.S., A.J. Alshaibani, and A.N. Abood, *Enhancing the loading capacity of kojic acid dipalmitate in liposomes.* Lat Am J Pharm, 2020. **39**(7): p. 1-7.
20. Achim, M., et al., *Thermosensitive liposomes containing doxorubicin. Preparation and in vitro evaluation. .* Revista Farmacia, 2009. **57**: p. 703-710.
21. Shawka Al-Asadi, L.J.A. and S. Al-Edresi, *REDUCTION OF TIME AND COST IN PREPARATION OF NANOFIBERS FROM PVA, PEO AND HPMC USING DESIGN-EXPERT® SOFTWARE.* International Journal of Applied Pharmaceutics, 2024. **16**(4): p. 257-266.
22. Huang, Z., et al., *Progress involving new techniques for liposome preparation.* Asian Journal of Pharmaceutical Sciences, 2014. **9**.
23. Kamra, M. and A. Diwan, *Liposomes In Dermatological Diseases.* Journal of Applied Pharmaceutical Research, 2017. **5**(2): p. 1-8.
24. Princely, S. and M. Dhanaraju, *Design, formulation, and characterization of liposomal-encapsulated gel for transdermal delivery of fluconazole.* Asian J Pharm Clin Res, 2018. **11**(8): p. 417-424.
25. Shilakari, G., D. Singh, and A. Asthana, *Novel vesicular carriers for topical drug delivery and their application's.* International Journal of Pharmaceutical Sciences Review and Research, 2013. **21**(1): p. 77-86.
26. Kamra, M. and A. Diwan, *Liposomes in dermatological diseases.* Journal of Applied Pharmaceutical Research, 2017. **5**(2): p. 01-08.
27. Mula, S., *IN-VITRO STUDY OF FORMULATION AND EVALUATION OF GLIMEPIRIDE NANOSUSPENSION BY PRECIPITATION METHOD.* World Journal of Pharmaceutical Research, 2020. **9**: p. 1239-1263.
28. Danaei, M., et al., *Impact of Particle Size and Polydispersity Index on the Clinical Applications of Lipidic Nanocarrier Systems.* Pharmaceutics, 2018. **10**(2): p. 57.
29. Di Francesco, M., et al., *Physicochemical characterization of pH-responsive and fusogenic self-assembled non-phospholipid vesicles for a potential multiple targeting therapy.* International Journal of Pharmaceutics, 2017. **528**(1): p. 18-32.
30. Madan, J.R., B.R. Adokar, and K. Dua, *Development and evaluation of in situ gel of pregabalin.* Int J Pharm Investig, 2015. **5**(4): p. 226-33.
31. Ahmed, T.A. and B.M. Aljaeid, *A potential in situ gel formulation loaded with novel fabricated poly(lactide-co-glycolide) nanoparticles for enhancing and sustaining the ophthalmic delivery of ketoconazole.* Int J Nanomedicine, 2017. **12**: p. 1863-1875.
32. Patel, C., et al., *Preformulation Study of Glimepiride: An Insight for Formulation and Development of Parenteral Formulation.* Journal of Pharmaceutical Research International, 2022. **34**(15B): p. 38-49.
33. Lakumalla, D., N. Podichety, and R. Maddali, *Design and characterization of glimepiride hydrotropic solid dispersion to enhance the solubility and dissolution.* Journal of Applied Pharmaceutical Research, 2024. **12**(2): p. 68-78.
34. Paul, A., et al., *Physicochemical Characterization, Molecular Docking, and In Vitro Dissolution of Glimepiride−Captisol Inclusion Complexes.* ACS Omega, 2020.
35. Kazi, M., et al., *Formulation and evaluation of glimepiride tablet by improving aqueous solubility of drug using hydrotropy technique.* World J. Pharm. Pharm. Sci., 2023. **12**: p. 1041-1054.
36. Seedher, N. and M. Kanojia, *Co-solvent solubilization of some poorly-soluble antidiabetic drugs.* Pharmaceutical Development and Technology, 2009. **14**(2): p. 185-192.
37. Mohd, A., et al., *Development and validation of RP-HPLC method for glimepiride and its application for a novel self-nanoemulsifying powder (SNEP) formulation analysis and dissolution study.* Journal of Analytical Science and Technology, 2014. **5**: p. (27)1-8.
38. Kishore, K., et al., *Preparation and characterization of oro dispersible tablets of glimepride-pvp k30 solid dispersion.* Int J Biol Pharm Res, 2013. **4**(8): p. 547-55.

39. Olusanya, T.O.B., et al., *Liposome formulations of o-carborane for the boron neutron capture therapy of cancer.* Biophysical Chemistry, 2019. **247**: p. 25-33.
40. Hashemzadeh, H., H. Javadi, and M.H. Darvishi, *Study of Structural stability and formation mechanisms in DSPC and DPSM liposomes: A coarse-grained molecular dynamics simulation.* Sci Rep, 2020. **10**(1): p. 1837.
41. Alfreahat, I., et al., *In Vitro Potentiation of Doxorubicin Cytotoxicity Utilizing Clarithromycin Loaded-PEGylated Liposomes.* Technol Cancer Res Treat, 2025. **24**: p. 15330338241312561.
42. Badran, M., *Formulation and in vitro evaluation of flufenamic acid loaded deformable liposomes for improved skin delivery.* Digest Journal of Nanomaterials & Biostructures (DJNB), 2014. **9**(1).
43. Anderson, M. and A. Omri, *The effect of different lipid components on the in vitro stability and release kinetics of liposome formulations.* Drug Deliv, 2004. **11**(1): p. 33-9.
44. Mandlik, S. and N. Ranpise, *Implementation of experimental design methodology in preparation and characterization of zolmitriptan loaded chitosan nanoparticles.* International Current Pharmaceutical Journal, 2017. **6**: p. 16.
45. Yen, T., et al., *Impact of Sample Concentration on the Determination of Particle Size of Nano Polymer Particles and Nano Liposomes by Dynamic Light Scattering.* VNU Journal of Science: Medical and Pharmaceutical Sciences, 2019. **35**.
46. Liu, T. and Y. Jiang, *The Application of Nanoparticle Concentration to the Evaluation of Liposome Physical Stability and Release Performance*, in *SSRN Preprints*. 2023.
47. Fadaly, W.A.A., et al., *Design, Synthesis and Biological Evaluation of Phenoxyacetic Acid derivatives Linked to Pyrazole Scaffold as PPAR-α/γ Agonists and COX-2 Inhibitors with Dual Antidiabetic/Anti-inflammatory Activities.* Journal of Molecular Structure, 2025. **1340**: p. 142578.
48. Martins, S., et al., *Physicochemical properties of lipid nanoparticles: effect of lipid and surfactant composition.* Drug Dev Ind Pharm, 2011. **37**(7): p. 815-24.
49. Manosroi, A., et al., *Chemical stability and cytotoxicity of human insulin loaded in cationic DPPC/CTA/DDAB liposomes.* J Biomed Nanotechnol, 2011. **7**(2): p. 308-16.
50. Zidan, A.S., et al., *Quality by design: Understanding the formulation variables of a cyclosporine A self-nanoemulsified drug delivery systems by Box–Behnken design and desirability function.* International Journal of Pharmaceutics, 2007. **332**(1): p. 55-63.
51. Rane, Y., et al., *Effect of hydrophilic swellable polymers on dissolution enhancement of carbamazepine solid dispersions studied using response surface methodology.* AAPS PharmSciTech, 2007. **8**(2): p. 27.